Differential leaf flooding resilience in *Arabidopsis thaliana* is controlled by age-dependent ORESARA1 activity

Tom Rankenberg[1,2], Hans van Veen[1,2], Mastoureh Sedaghatmehr[3], Che-Yang Liao[2,5], Muthanna Biddanda Devaiah[2], Salma Balazadeh[3,4], Rashmi Sasidharan[1,2]

1 – Plant Stress Resilience, Utrecht University; 2 – Plant-Environment Signaling; Utrecht University; 3 – Max Planck Institute of Molecular Plant Physiology; 4 – Leiden University; 5 – Laboratory of Biochemistry, Wageningen University

Keywords: flooding; abiotic stress; hypoxia; senescence; ethylene

Abstract

The volatile phytohormone ethylene is a major regulator of plant adaptive responses to flooding. In flooded plant tissues, it quickly increases to high concentrations due to its low solubility and diffusion rates in water. The passive, quick and consistent accumulation of ethylene in submerged plant tissues makes it a reliable cue to trigger flood-acclimative responses, including metabolic adjustments to cope with flood-induced hypoxia. However, persistent ethylene accumulation also accelerates leaf senescence. Stress-induced senescence hampers the photosynthetic capacity and stress recovery. In submerged *Arabidopsis* shoots, senescence follows a strict age-dependent pattern starting with the older leaves. Although mechanisms underlying ethylene-mediated senescence have been uncovered, it is unclear how submerged plants avoid an indiscriminate breakdown of leaves despite high systemic ethylene accumulation. Here we demonstrate in *Arabidopsis* plants that even though submergence triggers a leaf-age independent activation of ethylene signaling via EIN3, senescence was initiated only in the old leaves, and independent of the N-degron pathway of oxygen sensing. This EIN3 stabilization also led to the overall transcript and protein accumulation of the senescence-promoting transcription factor ORESARA1 (ORE1). ORE1 protein accumulated in both old and young leaves during submergence. However, leaf age-dependent senescence could be explained by ORE1 protein activation specifically in old leaves, independent of the previously identified age-dependent control of *ORE1* via miR164. Our results unravel a mechanism by which plants regulate the speed and pattern of senescence during environmental stresses like flooding. The age-dependent activity of ORE1 ensures that older expendable leaves are dismantled first, thus prolonging the life of younger leaves and meristematic tissues vital to whole plant survival.

Significance statement

Flooded plants systemically accumulate saturating concentrations of the senescence promoting volatile hormone ethylene. Yet, leaf senescence follows a strict age-dependent gradient, thus prolonging the survival of young leaves and meristematic tissue. Here we show that in flooded plants, age-independent activation of ethylene signaling via EIN3, induces the systemic accumulation of the senescence-inducing transcription factor ORE1. Premature senescence of younger tissues is prevented by the posttranslational activation of ORE1 specifically in old leaves, where it induces the transcription of senescence-associated genes. Our results highlight how a systemic stress signal (ethylene

accumulation upon flooding) induces a signaling cascade that diverges in an age-dependent manner, and eventually leads to an age-dependent physiological output (leaf senescence).

Introduction

Ethylene is a gaseous hormone that controls many aspects of plant development and is a central regulator of plant environmental stress responses (Dubois et al., 2018; Sasidharan and Voesenek, 2015). Plant endogenous ethylene concentrations increase in response to a wide variety of abiotic stresses primarily mediated by enhanced ethylene biosynthesis (Argueso et al., 2007). Subsequently, ethylene triggers the stabilization of the key transcription factor ETHYLENE-INSENSITIVE1 (EIN3) leading to downstream transcriptional cascades culminating in various stress responses (Chang et al., 2013; Binder, 2020).

Flooded plants present an exception to the stress-mediated increase in ethylene biosynthesis. At least immediately following flooding, ethylene levels rapidly increase in submerged plant tissues due to physical entrapment by the surrounding flood water. This quick increase of gaseous ethylene to physiologically saturating concentrations is a consequence of the severely limited gas diffusion underwater (Xie et al., 2015; Hartman et al., 2019; Voesenek and Sasidharan, 2013). The ethylene accumulation and consequent stabilization of EIN3 is used by plants as an early flooding signal. Ethylene is a major regulator of flood adaptive traits and influences performance during flooding in various ways. For example, in deepwater rice, ethylene signaling induces stem elongation during submergence by inducing gibberellin biosynthesis and signaling (Métraux and Kende, 1983; Hattori et al., 2009; Kuroha et al., 2018). In lowland rice, on the other hand, ethylene signaling represses shoot elongation and carbohydrate consumption via SUB1A (Xu et al., 2006; Fukao et al., 2006; Fukao and Bailey-Serres, 2008). In Arabidopsis, ethylene signaling aids transcriptional responses to flood-induced tissue hypoxia, inhibits growth and modulates damage caused by reactive oxygen species (ROS) to enhance hypoxia survival (Peng et al., 2001; Liu et al., 2022; Hartman et al., 2019; Tsai et al., 2014).

The characterization of the functions of ethylene in plant flooding responses has primarily focused on traits that aid survival. However, considering its well-established role as a positive regulator of senescence (Graham et al., 2012), ethylene accumulation likely accelerates leaf senescence during submergence. Leaf senescence is often considered a marker for flood sensitivity, as flooding-intolerant accessions of rice, Arabidopsis, maize, and *Lotus japonicus* display more severe leaf senescence during flooding and post-flooding compared to tolerant accessions (Alpuerto et al., 2016; Krishnan et al., 1999; Yeung et al., 2018; Campbell et al., 2015; Buraschi et al., 2020). Furthermore, Arabidopsis mutants with reduced senescence exhibit improved performance after submergence compared to wild-type plants (Zhang et al.; Yeung et al., 2018).

The response of plant tissues to ethylene strongly depends on the age of the tissue (Doubt, 1917; Chen et al., 2013; Ceusters and Van de Poel, 2018). Ethylene treatment induces senescence much faster in older leaves than in younger leaves (dela Fuente and Leopold, 1968; Jing et al., 2005). This ensures senescence and death occur only when a leaf has reached maturity. Some mechanisms have been identified that contribute to this age-dependent response to ethylene. As a leaf ages, *EIN3* transcription gradually increases, intensifying the strength of the response to endogenous ethylene (Li et al., 2013). EIN3 induces the transcription of the master senescence regulator *ORESARA1* (*ORE1*) a NAC transcription factor, the activity of which is controlled by the kinase CALCIUM-DEPENDENT PROTEIN KINASE1 (CPK1) (Durian et al., 2020). However in young leaves premature senescence is prevented due to the degradation of *ORE1* mRNA by the microRNA *miR164* (Kim et al., 2009). As a leaf ages, the abundance of *miR164* decreases, which leads to a gradual accumulation of *ORE1*. This gradient in *miR164* works as a buffer that prevents untimely senescence in young leaves. However, increased ethylene production in stressed plants can accelerate senescence even in young leaves.

In submerged Arabidopsis rosettes that would experience systemic accumulation of ethylene, senescence still occurs along a strict leaf age-dependent gradient. Here we investigated the underlying mechanisms of this sequential leaf death. We first established that this pattern was dependent on ethylene sensing but did not require hypoxia sensing via the N-degron pathway, which is another important signaling cascade for flood acclimation. Next, we found that ethylene signaling is activated in a leaf age-independent manner upon submergence and via EIN3, induces the accumulation of the senescence-regulating transcription factor ORESARA1 (ORE1), indicating a *miR164*-independent mechanism. Although ORE1 protein was present in old and young leaves during submergence, ORE1 activation and senescence was triggered only in old leaves due to age-dependent phosphorylation of ORE1 in these tissues, independent of *CPK1*. This age-dependent phosphorylation of ORE1 ensures that leaf senescence during flooding follows an age-dependent gradient, preventing systemic tissue degradation and prolonging shoot survival.

Results

<u>Ethylene perception during submergence is systemic but mediates age-dependent leaf death</u>

Arabidopsis plants (10 leaf stage) that were completely submerged (in the dark) for varying durations exhibited a typical age-dependent pattern of leaf death. This sequential leaf death started in the oldest leaves, progressing down the age gradient towards the youngest leaves and shoot apex, which died last (Figure 1A, supplemental video 1). Ethylene has been identified as an important regulator of both flooding responses and age-dependent stress responses (Sasidharan and Voesenek, 2015; Rankenberg et al., 2021; Ceusters and Van de Poel, 2018). It has previously been established that ethylene accumulates quickly in flooded tissues (Sasidharan and Voesenek, 2015) resulting in rapid stabilization of EIN3 (Xie et al., 2015; Hartman et al., 2019). EIN3 is a transcription factor that is a key regulator of downstream transcriptional responses to ethylene (Chao et al., 1997; Chang et al., 2013).

However, considering that the leaf death was not uniformly triggered across the submerged Arabidopsis rosettes, we wanted to establish whether ethylene signaling was indeed systemic. For this the levels of EIN3 protein were monitored in old and young leaves. Submergence enhanced EIN3 levels in both old and young leaves, already within a few hours consistent with the expected rapid accumulation of ethylene (Figure 1B). Interestingly, while EIN3 was stabilized rapidly following submergence, levels decreased thereafter during the first 24h of submergence. This is in agreement with previous observations of EIN3 as a hit-and-run transcription factor, binding briefly to its downstream targets, after which their transcription is maintained by other regulators (Alvarez et al., 2021; Chang et al., 2013). After establishing that ethylene signaling was activated systemically in flooded Arabidopsis plants, we investigated the role of ethylene in the observed leaf-age dependent senescence gradient. Age-dependent leaf death was quantified by dividing leaves into three categories based on their order of emergence: leaves 1 and 2, 3 to 5, and 6 to 8. Leaves were scored as dead when more than half of their blade area had desiccated after three days of post-submergence recovery and the proportion of dead leaves per category was calculated for each plant. This confirmed a significant leaf-age effect in wild-type plants (Figure 1C). However, this was lost in the ethylene-insensitive *ein3eil1* and *ein2-5* mutants (Figure 1C, 1D, S1B), indicating the involvement of ethylene signaling. We observed some variation between experiments in the speed at which leaves of submerged plants died. However, in all experiments the gradient in leaf death with age was consistently observed in plants that could respond to ethylene. In addition to ethylene, submergence especially during a light-limited flooding event also causes a significant decline in tissue oxygen levels (Vashisht et al., 2011; Sasidharan et al., 2018). To further probe the relative importance of ethylene in regulating the observed pattern of leaf death during submergence we exposed plants to combinations of the main submergence signals – ethylene, darkness, and hypoxia. The median hue of representative old (leaf 3) and young (leaf 7) leaves was used to quantify yellowing. The combination of ethylene and darkness induced age-dependent leaf yellowing, adding hypoxia to this combination ameliorated it (Figure 1E). However, hypoxia or darkness alone failed to trigger sequential leaf yellowing. Considering its established importance as a flooding stress cue we tested whether submergence-induced sequential leaf death requires hypoxia sensing. For this we used the Arabidopsis mutants *erfVII*, *pco124*, and *prt6-1* lacking important components of the plant oxygen sensing machinery (Abbas et al., 2015; Masson et al., 2019). In all these mutants, submergence still triggered the sequential leaf death pattern as observed in the wild type, suggesting that this response does not require oxygen sensing via the N-degron pathway (Figure 1F-H, S1B).

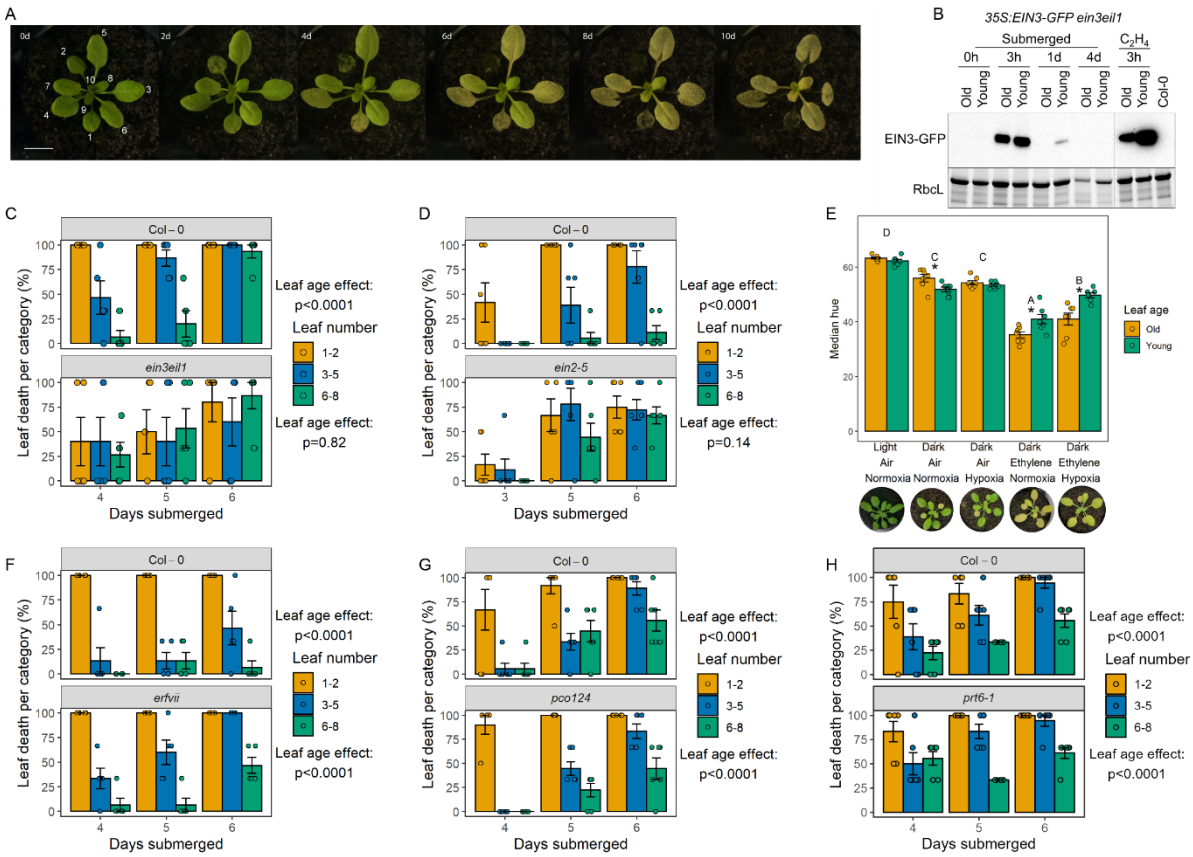

Figure 1 | Ethylene perception during submergence is systemic but mediates age dependent leaf death
A) Arabidopsis wild type (accession Col-0) plants submerged in darkness show age-dependent leaf death. Images are representative plants submerged for the duration indicated in the top-left of each image. Numbers in the first image indicate leaf numbers. Scale bar indicates 1cm.
B) Immunoblot analyses showing EIN3-GFP accumulates within 3h of submergence or ethylene treatment in both old (leaf 3) and young (leaf 7) leaves of transgenic *35S:EIN3-GFP ein3eil1* plants. Samples were run on the same gel; vertical line indicates where samples were cropped out. The large subunit of Rubisco (RbcL) served as a loading control.
C) and D) Quantification of leaf death across three age-categories of an Arabidopsis rosette. Age categories are indicated by leaf number as in Figure 1A. Age-dependent leaf death observed in wild-type plants is lost in ethylene-insensitive *ein3eil1* and *ein2-5* mutants. P-values indicate the effect of leaf age on the proportion of dead leaves per genotype, determined by a two-way ANOVA (leaf age * submergence duration). n=5-6 plants per timepoint.
E) The effect of different flooding cues on leaf yellowing in wild-type Arabidopsis plants. Yellowing is indicated by the median hue of old (leaf 3) and young (leaf 7) leaves, after four days of exposure to each treatment. Ethylene induces age-dependent leaf yellowing and this process is slowed down by hypoxia. Images below each bar show representative plants from each treatment. Asterisks indicate differences between old (leaf 3) and young (leaf 7) leaves (paired t-test), different letters indicate significant differences between treatments (two-way ANOVA + Tukey's post-hoc test). n=7 plants per treatment.
F - H) Age-dependent leaf death is not lost in *pco124*, *erfVII, and prt6-1* mutants, which have impaired oxygen sensing. P-values indicate the effect of leaf age on the proportion of dead leaves per genotype, determined by a two-way ANOVA (leaf age * submergence duration). n=5-6 plants per timepoint.

In conclusion, we confirmed that submergence-mediated sequential leaf death requires ethylene signaling. And, despite systemic activation of ethylene signaling in submerged rosettes, leaf death occurred in a more localized, defined pattern. The mechanisms underlying this observation were of interest to probe further.

157 Submergence-induced senescence is primarily controlled by the ethylene-responsive NAC-domain
158 transcription factor ORESARA1
159
160 The regulatory networks underpinning ethylene-mediated chlorophyll degradation leading to leaf
161 senescence and death are well-established (Woo et al., 2019). Of relevance for submergence-induced
162 senescence is the activation by ethylene of the NAC domain transcription factor ORESARA1 (ORE1)
163 (Qiu et al., 2015; Yeung et al., 2018). ORE1 is a positive regulator of leaf senescence. Since the
164 functioning of the EIN3-ORE1 regulon during leaf senescence is well-established, we used this as a
165 system to investigate how ethylene-mediated leaf senescence is coordinated in an age-dependent
166 manner during submergence (Kim et al., 2009; Li et al., 2013; Qiu et al., 2015).
167
168 Consistent with previous reports, ethylene-mediated senescence was reduced in *ore1-1* knockout
169 mutants (Figure 2A; (Li et al., 2013; Qiu et al., 2015)) and ethylene exposure triggered a substantial
170 increase in *ORE1* transcripts (Figure 2B). Interestingly, this increase was observed in both old and
171 young leaves.

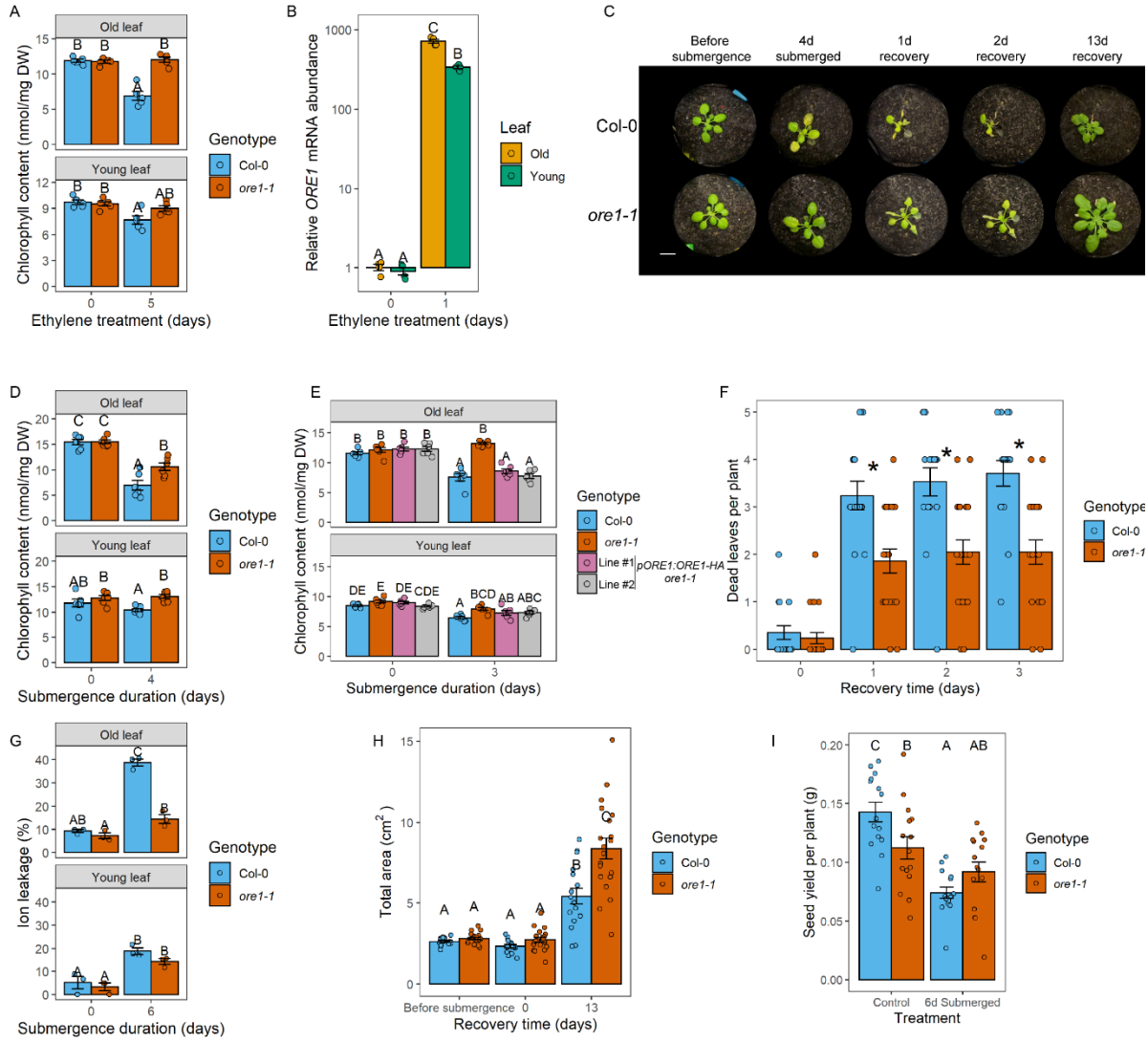

Figure 2 | Submergence-induced senescence is primarily controlled by the ethylene responsive NAC TF ORE1

A) Chlorophyll content of old and young leaves of Col-0 and *ore1-1* plants before and after 5 days of ethylene treatment. n=5 leaves per sample.
B) *ORE1* mRNA abundance increases in both old and young leaves after 1 day of ethylene treatment. n=4 leaves per sample, each consisting of 2 old or young leaves from different plants pooled together. Expression levels were normalized to those in old leaves of non-submerged plants.
C) *ore1-1* mutants show reduced yellowing of old leaves after 4 days of submergence. Representative images of Col-0 and *ore1-1* plants at the indicated timepoints. Scale bar indicates 1cm.
D) Chlorophyll content of old and young leaves of Col-0 and *ore1-1* before and after 4 days of submergence. n=6 leaves per sample.
E) Chlorophyll content of Col-0, *ore1-1*, and two independent *pORE1:ORE1-HA ore1-1* lines before and after 3 days of submergence. n=6 leaves per sample.
F) Dead leaves per Col-0 and *ore1-1* plant during recovery from 4 days of submergence. Leaves were scored as dead or alive at each of the indicated timepoints, n=17-21 plants per genotype. These same plants were phenotyped for figures S2E and S2H.
G) Ion leakage of Col-0 and *ore1-1* before and after 6 days of submergence. n=3 pools of 5 old or young leaves from different plants per sample.
H) Total living rosette area of Col-0 and *ore1-1* plants before and after 4 days of submergence, and after 13 days of recovery. Images of plants were categorised into dead, senescing, and healthy pixels using PlantCV. Senescing and healthy pixels were combined for each plant and converted to an area in cm^2. n=16-20 plants per sample.
I) Seed yield of Col-0 and *ore1-1* plants under control conditions and of plants that were submerged for 6 days. n=15 plants per group.
Different letters indicate significant differences between groups (two-way ANOVA + Tukey's post-hoc test). Asterisks indicate significant differences between Col-0 and *ore1-1* per timepoint.

172

173 Next, we set out to establish that ORE1 is indeed a principal regulator of submergence-induced
174 senescence. In accordance with its role as a positive regulator of senescence, submergence-induced
175 senescence was significantly reduced and enhanced in *ore1* mutants and overexpressors, respectively
176 (Figure 2C, 2D, S2A, S2B, S2C, Supplemental video 2). Moreover, the higher chlorophyll retention
177 phenotype of *ore1-1* mutants during submergence could be reverted to wild-type by complementation
178 with *ORE1* (ORE1 fused to an HA tag driven by its own promoter) (Figure 2E). ORE1 plays a role in
179 dark-induced senescence of detached leaves (Kim et al., 2018). We did not detect visual signs of
180 senescence in whole plants treated with darkness in the experimental duration used here (Figure 1D,
181 Figure S2D) and the effect of darkness on rosette area was not different between Col-0 and *ore1-1*
182 (Figure S2E). This shows that the submergence phenotype of *ore1-1* mutants is not merely a darkness
183 effect. In general, higher chlorophyll maintenance in *ore1-1* mutants corresponded with a better
184 performance during submergence relative to wild-type. This was reflected in a lower number of dead
185 leaves and lower electrolyte leakage, although there were no significant differences in the rate of new
186 leaf initiation immediately following desubmergence (Figure 2F, S2F, 2G, S2G). However, submerged
187 *ore1-1* mutants also displayed a greater retention of healthy rosette area, which led to a greater rosette
188 area after prolonged recovery (Figure S2H, 2H) and *ore1-1* seed yield was not compromised by flooding
189 (Fig 2I). Under control conditions, *ore1-1* mutants did have a significant reduction in seed yield
190 compared to wild-type plants. This can be attributed to delayed leaf senescence in *ore1-1* mutants. Leaf
191 senescence plays a vital role in remobilizing nutrients from dying leaves for seed production at the end
192 of a plant's lifecycle (Havé et al., 2017).
193
194 Notably, we found that the phenotype of *ore1* mutants was age-dependent: the reduction in leaf
195 senescence during flooding was most visible in old leaves (Figure 2C, S2A). Consistent with this visual
196 observation, the decrease in chlorophyll content and cell membrane integrity was the greatest in old

197 leaves of Col-0 plants (Figure 2D, 2G). We thus set out to investigate the regulation of ORE1 and
198 determine how it is activated in an age-dependent manner.
199
200 Leaf-age dependent regulation of ORE1
201 Submergence strongly enhanced *ORE1* transcript levels in whole rosettes and this effect was
202 maintained also during recovery. While darkness also triggered upregulation of *ORE1,* levels quickly
203 dropped as plants were placed back in the light (Figure 3A).

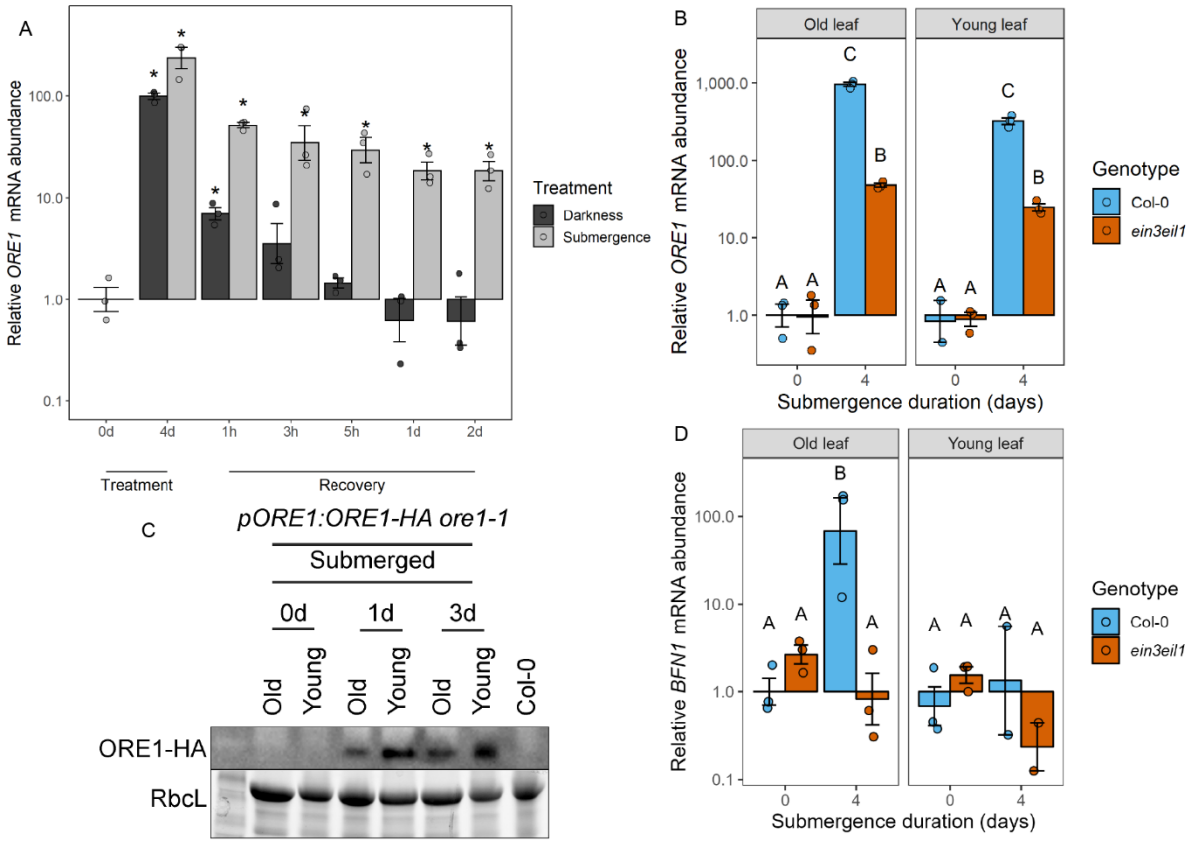

Figure 3 | *ORE1* is induced age-independently during flooding stress
A) *ORE1* mRNA abundance in whole rosettes before and after darkness and dark submergence. Asterisks indicate significant differences compared to untreated plants (one-way ANOVA + Dunnett's post-hoc test). Expression was normalized to that of untreated plants. n=3, each sample consists of one rosette.
B) *ORE1* mRNA abundance in old and young leaves before and after four days of submergence, in Col-0 and *ein3eil1*. Different letters indicate significant differences between groups (two-way ANOVA + Tukey's post-hoc test). Expression was normalized to that of non-submerged old leaves of Col-0. Three biological replicates were analysed, *ORE1* mRNA was not detected in one of the non-submerged Col-0 and *ein3eil1* young leaf samples; each sample consists of two leaves pooled together from different plants.
C) Immunoblots showing ORE1-HA protein abundance in old and young leaves before and after one and three days of submergence, using an antibody against HA. Each *pORE1:ORE1-HA ore1-1* sample consists of five old or young leaves pooled together from different plants. Proteins of the Col-0 sample are extracted from one whole rosette. The large subunit of Rubisco (RbcL) served as a loading control.
D) mRNA abundance of ORE1 target gene *BFN1* in old and young leaves before and after four days of submergence, in Col-0 and *ein3eil1*. Different letters indicate significant differences between groups (two-way ANOVA + Tukey's post-hoc test). Expression was normalized to that of non-submerged old leaves of Col-0. Three biological replicates were analysed, *BFN1* mRNA was not detected in one of the submerged Col-0 and *ein3eil1* young leaf samples; each sample consists of two leaves pooled together from different plants.

204 Surprisingly, submergence led to increased transcript levels of *ORE1* in both old and young leaves
205 (Figure 3B). This was further confirmed using a transgenic line in which the 1.6kb promoter of *ORE1*

206 was fused to a GUS enzyme. GUS staining patterns in both young and old leaves confirmed age-
207 independent *ORE1* promoter activity during flooding (Figure S3A). Next we examined whether age-
208 dependent differences in *ORE1* occur at the protein level. To do so, we complemented the *ore1-1*
209 mutant line with an HA-tagged version of ORE1, driven by its native 1.6kb promoter. In the
210 *pORE1:ORE1-HA ore1-1* lines, there was an accumulation of ORE1 protein in both old and young
211 leaves during submergence both at 1 and 3 days of submergence (Figure 3C). We did not detect any
212 ORE1 protein in either old or young leaves of non-submerged plants, as short-day grown Arabidopsis
213 plants at the 10-leaf stage have not yet initiated leaf senescence of their oldest leaves. Although *ORE1*
214 protein and mRNA accumulated in both old and young leaves during submergence, mRNA of the ORE1
215 target *BIFUNCTIONAL NUCLEASE1* only accumulated in old leaves (Figure 3D). *ein3eil1* mutants still
216 exhibited a modest increase in *ORE1* mRNA levels during submergence, but this did not lead to an
217 increase of *BFN1* mRNA levels (Figure 3D).
218
219 Ethylene is known to enhance *ORE1* mRNA abundance via two routes – a direct transcriptional
220 induction and via inhibition of its post-transcriptional repressor *miR164* (Kim et al., 2009). The latter
221 mode is associated with age-dependent ethylene-induced senescence. Young leaves typically have
222 high levels of *miR164* which decline with age. This ensures that *ORE1* mRNA is degraded when its
223 transcription is induced by EIN3 and protects young leaves from premature senescence (Kim et al.,
224 2009; Li et al., 2013). We did not observe significantly higher expression of *miR164b* in young leaves
225 compared to old leaves (Figure S3B), and the similar accumulation of ORE1 protein in both old and
226 young leaves (Figure 3C) suggests that the degradation of *ORE1* mRNA by *miR164* is not sufficient to
227 prevent premature accumulation of ORE1 protein during submergence.
228
229 <u>Despite systemic ORE1 accumulation, downstream targets are activated in a leaf age-dependent</u>
230 <u>manner</u>
231 Although ORE1 protein accumulated in old and young leaves during submergence (Figure 3C),
232 knocking out *ORE1* had a stronger effect on old leaves than on young leaves (Figure 2) and the ORE1
233 target *BFN1* was only induced in old leaves suggesting ORE1 activation only in these tissues (Figure
234 3D). To strengthen this evidence and get a global and unbiased overview of whether there is age-
235 dependent activation of ORE1 targets, we carried out an mRNA Seq experiment. Old and young leaves
236 of Col-0 and *ore1-1* were harvested before submergence, after 4 days of submergence, and after 6
237 hours of recovery (Figure 4A). Approximately 10 times as many differentially expressed genes (DEGs)
238 were found between old leaves of Col-0 and *ore1-1* than between young leaves during submergence
239 (Figure 4A). Interestingly, there were no genotype-specific DEGs when comparing the recovery
240 timepoint to the pre-submergence timepoint. Of the 720 genotype-specific DEGs in the recovery vs
241 submergence comparison, 428 were already differentially expressed after 4 days of submergence. This
242 suggests that knocking out *ORE1* mostly affects the transcriptome of old leaves during submergence
243 and not during recovery. Of the DEGs between the old leaves of Col-0 and *ore1-1* during submergence,
244 the subset that showed a smaller increase in expression during submergence in *ore1-1* than in Col-0
245 contained several previously identified targets of ORE1 including (*BIFUNCTIONAL NUCLEASE1*

(*BFN1*) and *NON-YELLOWING1* (*NYE1*)). Furthermore, these DEGs were enriched for ORE1 binding sites near their transcriptional start sites (Figure S4A). DEGs that did not fall within this subset did not have this enrichment, nor did non-DEGs.

We expanded the set of known ORE1 target genes by confirming that ORE1 can bind the promoters of the protease *METACASPASE9* (*MC9*), the transcription factor *ANAC010*, the nuclease *DEFECTIVE IN POLLEN ORGANELLE DNA DEGRADATION 1* (*DPD1*), and the chloroplast-degrading protein *CHLOROPLAST VESICULATION* (*CV*) *in vitro* via electrophoretic mobility shift assay (EMSA) (Figure 4B). These new targets were selected based on their roles in senescence-related processes. *In vivo* binding of ORE1 to these promoters was confirmed via ChIP-qPCR using 1-day submerged *pORE1:ORE1-HA* plants (Figure 4C). The binding of ORE1 to all newly identified putative targets was significantly enriched, when compared to the negative control (AT4G22180) (Figure 4C). Out of a set of 15 verified ORE1 targets, from this study and others ((Rauf et al., 2013; Matallana-Ramirez et al., 2013; Qiu et al., 2015; Zhang et al., 2021); Table S1), *ORE1* disruption affected the submergence-induction of 12 (in old leaves). In young leaves, however, only 3 out of the 15 differed in their response to submergence between Col-0 and *ore1-1* (Figure S4B).

The *ORE1*-dependent response during submergence does not seem to involve hypoxia signaling, as none of the 47 out of the 51 core hypoxia genes (HRGs) (Mustroph et al., 2009) detected in our dataset were different between Col-0 and *ore1-1* in either old or young leaves (Figure S2C). The mRNA Seq data also confirmed that global ethylene signaling was induced similarly in old and young leaves during submergence, based on the similar expression of EIN3 target genes between these leaves (Figure S4D).

269

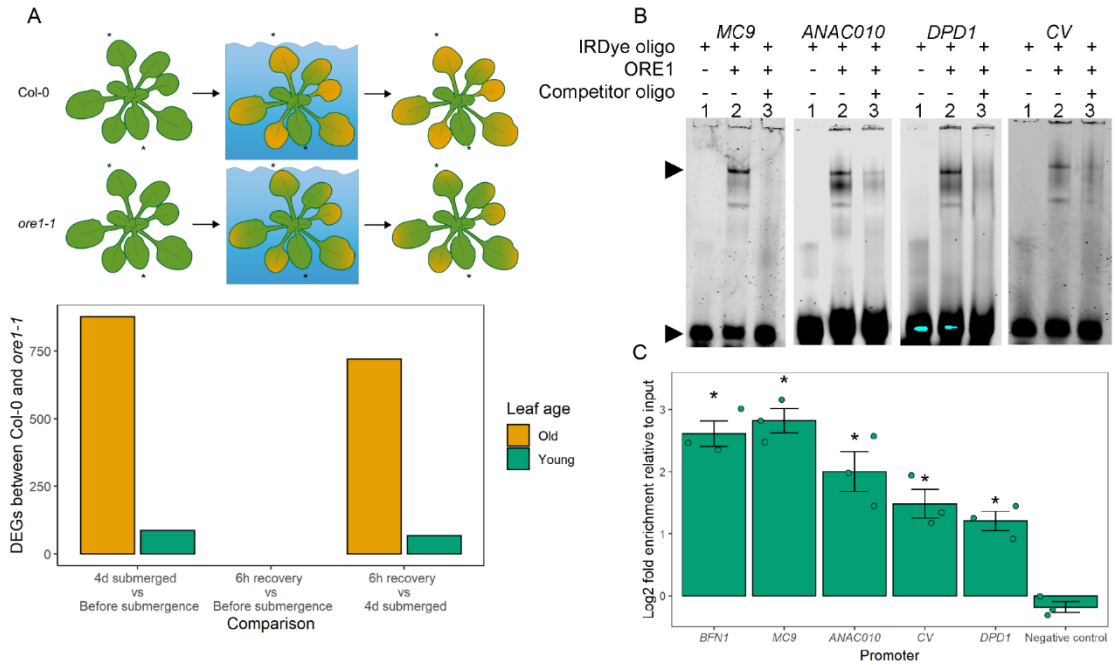

Figure 4 | ORE1 target activation is age-independent
A) Leaf samples of Col-0 and *ore1-1* were harvested before submergence, after four days of submergence, and after 6 hours of recovery. The number of differentially expressed genes (DEGs) that show a genotype-dependent response to four days of submergence is greater in old leaves than in young leaves. None showed a genotype-dependent effect in their response to submergence followed by recovery. Most (428/720) DEGs showing a genotype-specific response to post-submergence recovery showed the opposite pattern during the submergence phase.
B) Electrophoretic Mobility Shift Assay (EMSA) showing *in vitro* binding of recombinant ORE1-GST to the promoters of *MC9*, *ANAC010*, *DPD1*, and *CV*. From left to right in each image: lane 1, labeled probe (5′-DY682-labeled double-stranded oligonucleotides); lane 2, labeled probe plus ORE1-GST protein; lane 3, labeled probe, ORE1-GST protein, and competitor (unlabeled oligonucleotide containing an ORE1 binding site; 200× molar access). Arrows indicate retarded bands (bound oligo) and the non-bound DNA probes (free oligo).
C) ChIP-qPCR showing *in vivo* binding of ORE1 to the promoters of *MC9*, *ANAC010*, *DPD1*, and *CV*. Asterisks indicate significant enrichment relative to the negative control (AT2G22180) (one-way ANOVA + Dunnett's post-hoc test). Chromatin was extracted from immunoprecipitated samples from whole *pORE1:ORE1-HA* rosettes submerged for one day, n=3.

270 <u>Age-dependent ORE1 phosphorylation during submergence is required for downstream target</u>
271 <u>activation</u>
272 Although ORE1 protein accumulated to higher levels during submergence in young leaves than in old
273 leaves, its downstream targets were mostly activated in old leaves. This indicated an age-dependent
274 activation of ORE1 in old leaves. The transactivation ability of ORE1 was recently shown to depend on
275 its six-fold phosphorylation (Durian et al., 2020). We thus probed this post-translational modification as
276 a potential mechanism mediating differential ORE1 activation in our system. Protein extracts from
277 leaves of submerged *pORE1:ORE1-HA* plants run on an SDS-PAGE gel containing 50μM PhosTag
278 revealed a slower migration of ORE1-HA from old leaves. This suggested the presence of
279 phosphorylated ORE1-HA in old, submerged leaves supporting our hypothesis of age-dependent ORE1
280 activation via phosphorylation during submergence (Figure 5A). To further validate this, we used
281 transgenic plants overexpressing a modified ORE1 missing the region between amino acids 205 and
282 221 containing potential phosphorylation sites (*35S:ORE1Δ17)*. These *35S:ORE1Δ17* plants showed a
283 phenotype intermediate between Col-0 and *ore1-1* plants under submergence stress (Figure 5B, 5C).

As expected, the expression of *ORE1* was already high before submergence in *35S:ORE1* and *35S:ORE1Δ17* and was also induced in both old and young leaves of Col-0 and *ore1-1* leaves during

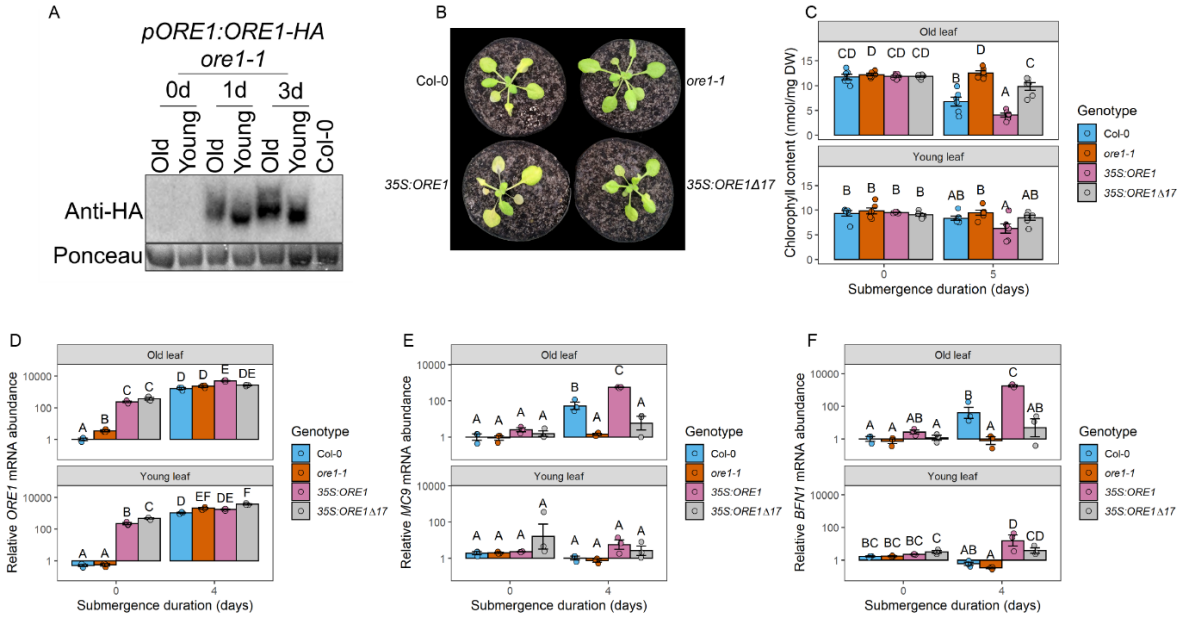

Figure 5 | ORE1 phosphorylation during flooding is age-dependent
A) *pORE1:ORE1-HA ore1-1* protein samples from submerged old leaves move slower through a PhosTag gel than samples from young leaves, indicating age-specific phosphorylation of ORE1. Five old or young leaves were pooled together from different plants per *pORE1:ORE1-HA ore1-1* sample, the Col-0 sample was from one whole rosette.
B) Representative images of Col-0, *ore1-1*, *35S:ORE1*, and *35S:ORE1Δ17* plants after 5 days of submergence followed by one day of recovery. Scale bar indicates 1cm.
C) Chlorophyll content of Col-0, *ore1-1*, *35S:ORE1*, and *35S:ORE1Δ17* plants, before and immediately after 5 days of submergence.
D-F) Expression of *ORE1*, *MC9*, and *BFN1* in Col-0, *ore1-1*, *35S:ORE1*, and *35S:ORE1Δ17* before and after 4 days of submergence. Expression was normalized to that of non-submerged old leaves of Col-0. Two old or young leaves from different plants were pooled together per sample. Different letters indicate significant differences between groups (two-way ANOVA + Tukey's post-hoc test). Error bars indicate SEM.

submergence (Figure 5D). The *ore1-1* mutant is a true null mutant containing a T-DNA insertion in the last exon. The primer pair used here spans the first intron, explaining the increase in *ORE1* transcript levels in *ore1-1* (Durian et al., 2020; Balazadeh et al., 2010). Although expression of *ORE1* was high during submergence in both old and young leaves of all four genotypes used here, the downstream target genes *MC9* and *BFN1* were only induced in the old leaves of Col-0 and *35S:ORE1* (Figure 5E-F). Taken together, these results suggest that the age-dependent phosphorylation of ORE1 is required for the activation of its downstream target genes.

<u>Ethylene exposure is sufficient to induce age-dependent accumulation of phosphorylated ORE1</u>

Plants with impaired ethylene signaling did not show age-dependent leaf death during submergence, and treating plants with ethylene in darkness induced age-dependent leaf death (Figure 1C-E). This could not be explained by *ORE1* transcript levels since ethylene treatment and submergence caused leaf-age independent *ORE1* induction (Figure 2B & 3B). This held true also for ORE1 protein levels (Fig 3C and Fig 6A). While the combination of ethylene and darkness was both essential and sufficient for the induction of ORE1 protein to similar levels as during submergence, this occurred in both old and

young leaves (Figure 6A). However, considering that during submergence ORE1 phosphorylation and activation occurred only in old leaves, we hypothesized that ethylene might be the underlying submergence signal (Figure 5A). In accordance with this, ethylene exposure in darkness was already sufficient to induce the accumulation of age-dependently phosphorylated ORE1 protein in one day (Figure 6B). This is consistent with the previous observation that ethylene treatment, rather than hypoxia, is sufficient to induce age-dependent leaf yellowing (Figure 1D). Furthermore, treating plants with ethylene in darkness had a similar effect on the senescence phenotype of Col-0 plants as submerging them in darkness (Figure 6C, 6D). In ethylene-insensitive *ein3eil1* plants, however, this induction of senescence during dark submergence was lost. To probe this further, we induced *ORE1* expression throughout the rosette by using transgenic plants expressing *ORE1* under an estradiol-responsive promoter. Systemic *ORE1* induction led to an age-dependent induction of its target genes and age-dependent leaf yellowing (Figure S5). This suggests that flooding-induced ethylene signaling controls the systemic ORE1 accumulation but is not essential for the age-dependent activation of ORE1. The loss of age-dependent senescence observed in flooded ethylene-insensitive mutants (Figure 1), could likely be an effect of the role of ethylene in leaf development (Vandenbussche et al., 2012).

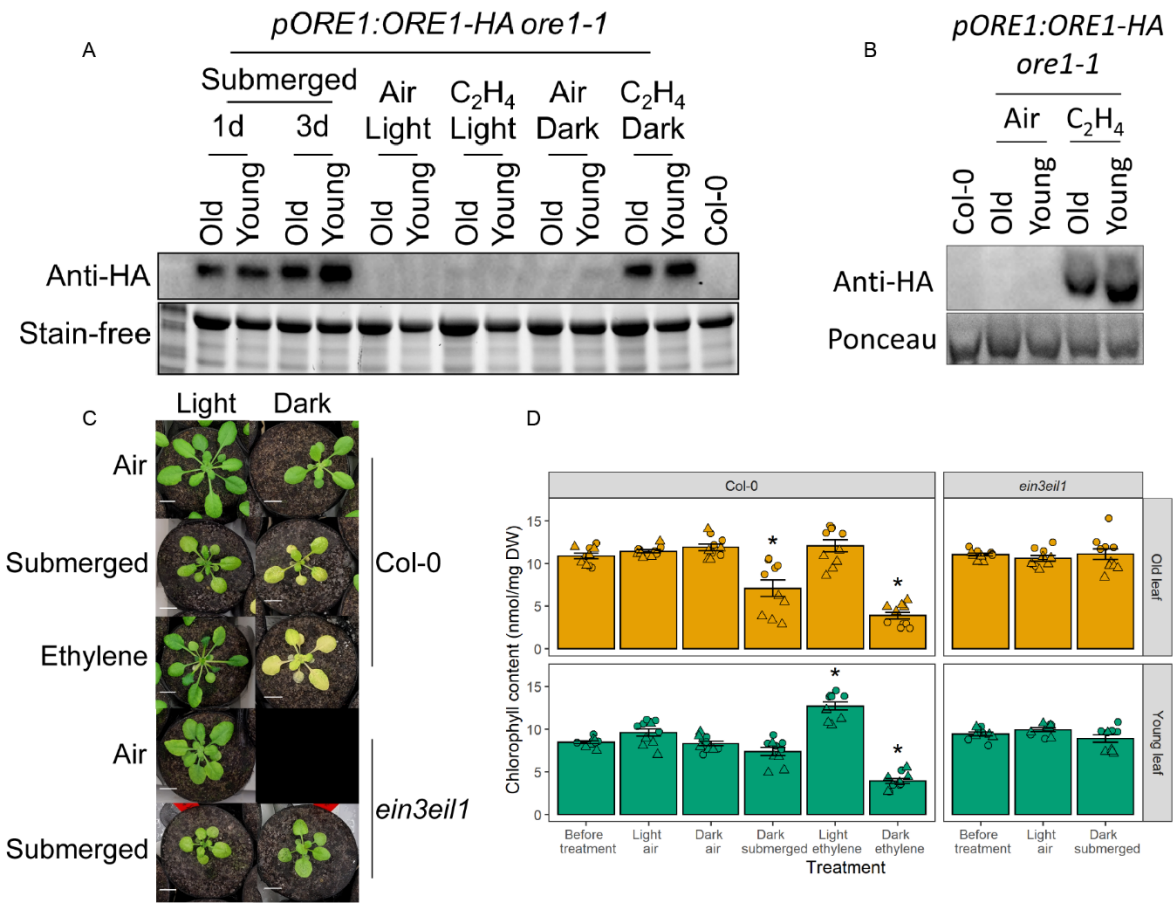

Figure 6 | Ethylene controls leaf age-dependent ORE1 phosphorylation
A) Immunoblots showing ORE1 accumulation in old and young leaves after submergence or one day of ethylene treatment in darkness. Five old or young leaves from different plants were pooled together per *pORE1:ORE1-HA ore1-1* sample. The Col-0 sample was from one whole rosette. Stain-free imaging of the protein gel was used as a loading control.
B) ORE1-HA from old leaves treated with ethylene in darkness for one day moves slower through a phostag gel than ORE1-HA from young leaves. Samples are the same as the ones run on the non-phostag gel in panel A. Ponceau staining of the large subunit of Rubisco was used as a loading control.
C) Shoot phenotypes in response to submergence or ethylene in light or dark conditions. Representative images of Col-0 and *ein3eil1* plants immediately after five days of the indicated treatments are shown. Scale bars indicate 1cm.
D) Chlorophyll content of old and young leaves following treatments with different combinations of ethylene and darkness. Asterisks indicate significant differences from chlorophyll levels before the treatment (One-way ANOVA + Dunnett's test), error bars indicate SEM. n=10 per sample from two independent experiments, circles and triangles indicate experimental replicates.

ORE1 is phosphorylated by CPK1 *in vivo* (Durian et al., 2020). *CPK1* mRNA levels showed a leaf age-dependent increase in submerged plants, although the absolute changes in expression are small (Figure S6A). *CPK1* also possessed an EIN3 binding site in its promoter (Figure S6B). We thus investigated it as a candidate kinase that phosphorylates and activates ORE1 downstream of ethylene. However, *CPK1* expression did not change in response to ethylene treatment in either old or young leaves (Figure S6C). Consistent with this, chlorophyll content of *cpk1-1* mutants was not different from Col-0 after either submergence or ethylene treatment (Figure S6D-E). A comparison of Col-0, *ore1-1*, and *cpk1-1* plants revealed age-dependent leaf death in all genotypes upon submergence. This was significantly delayed in *ore1-1* compared to Col-0 but not in *cpk1-1* (Figure S6F). Thus, although

327 ethylene exposure selectively induces senescence in old leaves via the age-dependent phosphorylation
328 of ORE1, this does not seem to depend on *CPK1*.
329
330 Taken together, these results provide a mechanism by which plants ensure that leaf senescence follows
331 an age-dependent gradient during flooding stress. Such a mechanism might safeguard a total overall
332 collapse of the plant due to high ethylene accumulation during flooding. Interestingly it is still unclear
333 what prevents ethylene-mediated activation in young leaves. Although flooding stress induces systemic
334 ethylene signaling and ORE1 accumulation, the age-dependent phosphorylation of ORE1 ensures that
335 it can only activate its downstream targets in older tissues (Figure 7). The accumulation of ORE1 in
336 young leaves can prepare them to rapidly transition into senescence if the submergence duration is
337 long enough.

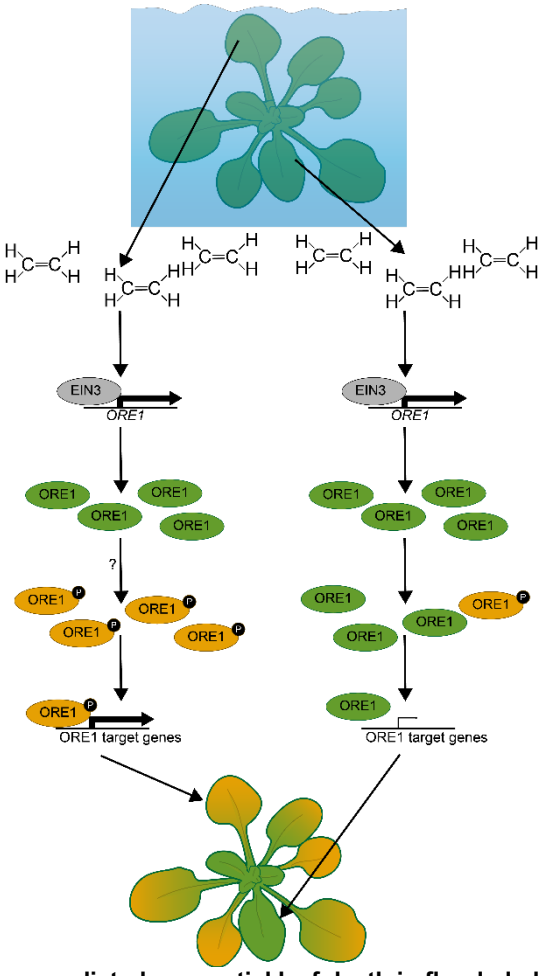

Figure 7 | A model for ethylene-mediated sequential leaf death in flooded plants.
Upon submergence, ethylene rapidly accumulates throughout a plant. This age-independent accumulation of ethylene induces the age-independent accumulation of *ORE1* mRNA and protein via EIN3 stabilization. Leaf-age dependent senescence is triggered by ethylene via ORE1 phosphorylation and activation specifically in old leaves, via an unknown mechanism. This age-dependent phosphorylation of ORE1 ensures that it induces senescence in old leaves, which results in the oldest leaves being broken down first and the youngest leaves and meristem last.

338
339 **Discussion**

340 Our results demonstrate a mechanism whereby plant responses to a systemic stress cue are locally
341 determined. Submergence of Arabidopsis rosettes activates ethylene signaling in all leaves, consistent
342 with an expected systemic accumulation of ethylene and yet initiates senescence in a specific leaf-age
343 dependent pattern. Leaf senescence during flooding starts in the oldest leaves, but eventually spreads
344 down the age gradient to younger leaves. Ethylene accumulation and signaling throughout the plant
345 causes this age gradient, whereby the transcription factor ORE1 plays a dominant role in rapidly starting
346 the de-greening process preferentially in older leaves. Though ethylene leads to ORE1 protein
347 accumulation independent of age, ORE1 activation via phosphorylation occurs specifically in the older
348 leaves. Such a mechanism ensures ORE1 target activation and senescence only in these older leaves.
349 Although ORE1 protein was already produced in young leaves within one day of submergence, its
350 effects on the transcriptome were minimal during 4 days of submergence. The premature production of
351 ORE1 in young leaves means that during prolonged submergence, when energy levels are low,
352 senescence can be induced without the need to make new ORE1 protein. In such an instance ORE1
353 only needs to be phosphorylated to induce the transcription of its downstream targets.

354 ORE1 is arguably one of the best-studied transcription factors controlling leaf senescence in
355 Arabidopsis. Transcription of *ORE1* is, besides EIN3, directly induced by other transcription factors
356 including ATAF1, ATAF2, PIF4, PIF5, ABI5, EEL, PRR9, WRKY71, GI, and ARF2 (Garapati et al., 2015;
357 Nagahage et al., 2018; Sakuraba et al., 2014; Kim et al., 2018; Yu et al., 2021; Kim et al., 2020; Xue et
358 al., 2022). *ORE1* mRNA levels are regulated post transcriptionally by *miR164* (Kim et al., 2009). The
359 low *ORE1* mRNA levels in old leaves under control conditions (Figure 2B & 3B) despite the strong
360 *ORE1* promoter activity (Figure S3B) suggest that *ORE1* mRNA was rapidly broken down, potentially
361 via miR164. ORE1 protein levels are controlled by ubiquitination by the E3 ligase NLA and the E2
362 conjugase PHO2, and by deubiquitination by the ubiquitin-specific proteases UBP12 and UBP13 (Park
363 et al., 2018, 2019). Lastly, the transactivation activity of ORE1 is activated via its phosphorylation by
364 CPK1 (Durian et al., 2020). The established pathway of miR164-based inhibition of premature ORE1
365 accumulation was not sufficient to prevent the accumulation of ORE1 in young leaves during flooding.
366 Despite the plethora of regulators that affect the abundance of *ORE1* mRNA and protein, we found that
367 ORE1 abundance does not explain the difference in ORE1 target gene activation between old and
368 young leaves during submergence. Rather, this difference is controlled by post-translational
369 modification of ORE1, which limits its activity to old leaves. ORE1 induces the transcription of its targets
370 via an interaction with the positively charged C-terminus of Mediator complex subunit 19a (MED19A),
371 which recruits RNA Polymerase II to target genes (Cheng et al., 2022). Phosphorylation of a protein
372 typically reduces its charge, and the phosphorylation of ORE1 could potentially facilitate its binding to
373 MED19a. This is also consistent with the impaired transactivation activity of ORE1Δ17, although it still
374 exhibits DNA binding activity (Durian et al., 2020).

375 Ethylene can freely diffuse across cell membranes and does not require specific transporters to move
376 between cells. The lack of control of ethylene movement requires a plant to have a highly tissue-specific
377 response system to ethylene. This has been described for different cell types (Vaseva et al., 2018;
378 Polko et al., 2011; Cao et al., 1999; Rajhi et al., 2011), but also for similar tissues in different

379 developmental stages (Jing et al., 2005; dela Fuente and Leopold, 1968). Tissue-specific regulation of
380 ethylene responsiveness occurs on many different levels of the ethylene signaling cascade (Stepanova
381 and Alonso, 2009). Since ethylene-insensitive mutants do not induce ORE1-mediated senescence of
382 old leaves during flooding, their old leaves die slower than those of wild-type plants. The young leaves
383 of ethylene-insensitive mutants, on the other hand, die faster than those of wild-type plants. This could
384 be an effect of the impaired ability of ethylene mutants in responding to reactive oxygen species that
385 accumulate during submergence recovery or of other unidentified roles of ethylene in submergence
386 survival (Tsai et al., 2014; Liu et al., 2022). This highlights how ethylene signaling can lead to either the
387 death or survival of a leaf during flooding stress, depending on the age of the leaf.

388 Our results show that ethylene-induced leaf senescence requires darkness. It is currently unclear if this
389 is an effect of light signaling or of darkness-induced carbon starvation, as both are known to interact
390 with ethylene signaling (Zhong et al., 2012; Shi et al., 2016; Yanagisawa et al., 2003; Kim et al., 2017).
391 In addition to ethylene accumulation, impaired gas diffusion also leads to a decline in oxygen levels in
392 flooded plants. Hypoxia is also considered an important regulatory signal mediating flood survival
393 responses. Hypoxia by itself does not impose a gradient of age-dependent leaf yellowing, and mutants
394 with impaired hypoxia sensing still show age-dependent leaf death during flooding stress (Figure 1D-
395 F). Furthermore, core hypoxia genes are not affected by the loss of *ORE1*, showing that *ORE1* is not
396 upstream of hypoxia signaling (Figure S4D). Based on these results we conclude that the sequential
397 leaf death described here does not appear to involve oxygen sensing and signaling. ORE1 and rice
398 SUB1A are both important regulators of the response to submergence, but both of them are primarily
399 controlled by ethylene rather than hypoxia (Gibbs et al., 2011; Lin et al., 2019). This likely stems from
400 the prevalence of hypoxia in normal plant development and the variation in oxygen concentrations
401 among submerged plant tissues (Weits et al., 2019; Sasidharan et al., 2018).
402
403 Ethylene accumulation upon submergence induces senescence of old leaves via the age-dependent
404 phosphorylation of ORE1. Our results suggest that this phosphorylation is independent of CPK1, which
405 is known to phosphorylate ORE1 in vivo (Durian et al., 2020). Future research should focus on how
406 exactly the age-dependent phosphorylation of ORE1 is controlled. Protein kinases and phosphatases
407 themselves are often controlled post-translationally and the interactions between them and their targets
408 can be highly context-specific (Simeunovic et al., 2016; Bhaskara et al., 2019), potentially complicating
409 the identification of the posttranslational regulators of ORE1 during submergence.
410
411 The severely reduced diffusion of gases in water means that ethylene will accumulate rapidly in any
412 plant tissue that is completely submerged. This property of ethylene makes it an ideal flood warning
413 cue mediating many flood-adaptive traits (Sasidharan and Voesenek, 2015). However, such high
414 concentrations of ethylene mean that senescence is inevitable for submerged leaves. Therefore, a
415 mechanism that prevents the simultaneous indiscriminate breakdown of all leaf tissue in such a situation
416 is essential to prolong survival. During natural plant ageing, the genetically coordinated process of
417 chlorophyll breakdown during senescence serves to remobilize nutrients towards seed and tuber filling
418 (Yu et al., 2015). The ability to retain chlorophyll has been found to correlate with higher tolerance to

419 submergence and improved post-submergence photosynthesis (Alpuerto et al., 2016; Yeung et al.,
420 2018). For example, the submergence tolerance gene *SUB1A* delays leaf senescence. Like *ORE1*, the
421 expression of *SUB1A* is regulated by ethylene (Fukao et al., 2006). Whereas ORE1 induces chlorophyll
422 degradation, *SUB1A* inhibits it during both submergence and darkness, and thereby contributes to a
423 quiescence strategy during flooding (Xu et al., 2006; Fukao et al., 2006, 2012). However, during
424 prolonged submergence as energy reserves become increasingly limited, senescence would be a
425 beneficial option. In such a situation, a sequential dismantling of older leaves would make available
426 energy and nutrient reserves that can be redirected to sustain younger leaves and the meristem. This
427 sacrificial use of older leaves would serve to enhance growth and photosynthesis recovery when
428 floodwaters subside. Understanding how plants coordinate which tissues are broken down under
429 stressful conditions could help in developing more stress-tolerant crop varieties, as the role of NAC
430 domain transcription factors in senescence is conserved across many plant species (Podzimska-Sroka
431 et al., 2015).
432
433
434
435
436 **Methods**
437
438 Plant material

439 *ore1-1* (SALK_090154): described in (He et al., 2005). Ordered from NASC

440 *ore1-2* (SAIL_694_C04): described in (Kim et al., 2020). Ordered from NASC

441 *cpk1-1* (SALK_096452): described in (Durian et al., 2020). Ordered from NASC

442 *35S:ORE1*: described in (Matallana-Ramirez et al., 2013). Gift from Salma Balazadeh

443 *35S:ORE1Δ17*: described in (Durian et al., 2020). Gift from Salma Balazadeh

444 *ein2-5*: described in (Alonso et al., 1999). Ordered from NASC

445 *ein3eil1*: described in (Alonso et al., 2003). Ordered from NASC

446 *pco124*: described in (Masson et al., 2019). Gift from Daan Weits

447 *erfVII*: described in (Abbas et al., 2015). Gift from Daan Weits

448 *prt6-1*: described in (Garzón et al., 2007). Gift from Angelika Mustroph

449 *35S:EIN3-GFP ein3eil1*: described in (Xie et al., 2015). Gift from Shi Xiao

450 RPS5a::XVE>>ORE1-GFP: Described in (Gao et al., 2018). Gift from Moritz Nowack

451 *pORE1:ORE1-HA ore1-1*: this study

452 *pORE1:GUS*: this study

453 All *Arabidopsis thaliana* (Arabidopsis) lines were in the ecotype Col-0 (Columbia-0) background

454

455 Generating transgenic lines

456 Genomic DNA from an Arabidopsis ecotype Col-0 leaf was extracted using phenol:chloroform:isoamyl
457 alcohol. The *ORE1* genomic region, including introns, 5'UTR, and a 1624bp promoter, was amplified
458 from this DNA using primers 5383 & 5384 (Supplemental table 2) and inserted into the pJET1.2 vector
459 (Thermo Fisher, K1231) according to the manufacturer's instruction. For the *pORE1:ORE1-HA* line the
460 entire fragment without the stop codon was amplified from this vector using primers 5383 & 5510, and
461 the HA tag was added using primers 5383 & 5783. For the *pORE1:GUS* line the *ORE1* promoter was
462 amplified using the primers 5383 & 5712. Adapters for binary LIC vectors pPLV01 and pPLV13 (De
463 Rybel et al., 2011) were added to the *pORE1:ORE1-HA* and *pORE1* fragments using primers 5804 &
464 5761 and 5739 & 5740, respectively. The fragments were inserted into their respective vectors via
465 ligation-independent cloning as described in (De Rybel et al., 2011). These vectors were introduced
466 into *Agrobacterium tumefaciens* strain AGL-1 via electroporation, and *ore1-1* and Col-0 Arabidopsis
467 plants were transformed using the floral dip method (Logemann et al., 2006). Independent T_1
468 transformants were selected on plates containing 50µM Basta/PPT, homozygous T_3 or T_4 lines were
469 used in all experiments.

470

471 Plant growth & treatments

472 Seeds were sowed on Primasta soil mix and stratified in the dark for 3 to 4 days before being transferred
473 to a short-day condition climate chamber (20C, 9h light 15h dark, 70%RH, ~140-180PAR either LED or
474 fluorescent light). After germinating for nine days, seedlings were transplanted to individual (5.5cm
475 diameter, 5cm height) pots consisting of 2:1 perlite:soil mix, which were covered with a black mesh to
476 prevent soil from floating out of the pot during submergence. 1 liter of 0.5x Hoagland medium was
477 added to each tray of 42 pots. When plants reached the 10-leaf stage they were submerged in complete
478 darkness at 20C for the indicated amount of time, and were left to recover for the indicated amount of
479 time in the original climate chamber. Submergence treatment for the timelapse videos (Supplemental
480 videos 1 & 2) was done at 1 PAR, pictures were taken every 30 minutes over two weeks using a Nikon
481 D750 camera. Ethylene treatments were done in 22.5l desiccators as described in Hartman et al.
482 (2019). Hypoxia treatments were done by mixing N_2 and air to a concentration of 5% O_2, which was
483 flushed through a desiccator for 1h. Desiccator valves were then closed and 5-10ppm ethylene was
484 injected with a syringe. For leaf death quantification, leaves were scored as dead when more than half
485 of the leaf area had desiccated after 3 days of post-submergence recovery in the light.

486

487 Green and senescing leaf area quantification

488 Pictures of Col-0 and *ore1-1* plants were taken with a Nokia 8 phone camera. Individual pixels in each
489 picture were classified into either "green", "senescing", "dead", or "background" using the "Naïve Bayes
490 Multiclass" module within PlantCV (Fahlgren et al., 2015). ImageJ was used to count the amount of
491 pixels in the green and senescing categories, and this was plotted relative to the amount of green pixels
492 before the start of treatment for Figure S2H. For Figure 2H the amount of green and senescing pixels
493 of the same plants were added together and converted into an area in cm^2.

494

495 Seed yield

496 For seed yield measurements, plants were either kept in short-day control conditions or submerged for
497 6 days in darkness and then returned to control conditions. Watering was stopped once the first siliques
498 started to dry out and plants were left to dry out until all siliques had ripened.

499

500 Chlorophyll quantification

501 For chlorophyll measurements, individual old or young leaf blades of the indicated genotypes were cut
502 off and put into 1.5ml Eppendorf tubes containing 1ml DMSO at the indicated timepoints. Tubes were
503 incubated in a shaking water bath at 60C for 30 minutes in darkness, and were then left to cool down
504 to room temperature for another 30 minutes in darkness. 200µl of each DMSO solution was pipetted
505 into a 96-well plate and absorption was measured at 647nm, 664nm, and 750nm using a
506 spectrophotometer plate reader (Synergy HT Multi-Detection Microplate Reader; BioTek Instruments).
507 Chlorophyll A was calculated as 13.71*(664nm-750nm)-2.858*(647nm-750nm), chlorophyll B was
508 calculated as 22.39*(647nm-750nm)-5.42*(664nm-750nm). Leaves were dried at 80C for 48h before
509 measuring their dry weight on a Mettler-Toledo MX5 microbalance. Total chlorophyll was calculated by
510 adding chlorophyll A and B together and dividing them by the measured dry weight.

511

512 Ion leakage

513 Five leaves per replicate of indicated tissues were pooled together in a 15ml tube containing 3ml distilled
514 water, and were gently shaken for 3 hours. The concentration of ions in the solution was measured
515 using a Horiba EC-33 conductivity meter. Plant tissue was then boiled for 20 minutes to destroy all
516 membranes, and ion leakage was measured again to determine the total ion content. Relative ion
517 leakage was calculated as the proportion of the conductivity before boiling to the conductivity after
518 boiling.

519

520 Gene expression

521 RNA was extracted from the indicated tissues using the Qiagen plant RNeasy mini kit, including an on-
522 column DNAse treatment, according to the manufacturer's instructions. qPCR data shown in figures 3B
523 and S3B was done using the Spectrum RNA extraction kit (Sigma-Aldrich), followed by DNase
524 treatment using AMPD1 DNase I (Sigma-Aldrich) to ensure that *miR164b* would not be excluded by the
525 size exclusion limit of the Qiagen kit.

526 Extracted RNA was converted into cDNA using RevertAid H Minus Reverse Transcriptase (Thermo
527 Scientific). For qPCR 20ng of cDNA was used per 5µl reaction, using SYBR Green master mix (BioRad)
528 and the primers indicated in Supplemental table 1.

529

530 GUS staining

531 Whole rosettes of 10-leaf *pORE1:GUS* plants were cut off at the indicated timepoints and were fixated
532 in 90% acetone for 20 minutes. Plants were then washed twice for 10 minutes in GUS washing buffer
533 (0.1M phosphate buffer pH=7, 10mM EDTA, 2mM $K_3Fe(CN)_6$) under vacuum. Plants were then stained
534 with GUS washing solution (0.1M phosphate buffer pH=7, 10mM EDTA, 1mM $K_3Fe(CN)_6$, 1mM
535 $K_4Fe(CN)_6$*3H2O, 0.5mg/ml X-Gluc) for 10 minutes under vacuum, followed by 20 hours at 37C.
536 Staining was stopped by incubating the plants with 3:1 acetic acid:ethanol for 1h, and were cleared by
537 washing with 70% ethanol. Plants were scanned using an Epson V800 scanner.

538 RNA sequencing

539 Between 8 and 16 young and old leaves of Col-0 and *ore1-1* were harvested before submergence, after
540 4 days of dark submergence, and after 6 hours of post-submergence recovery in the light. Additional

541 Col-0 samples were harvested after 2 days (old and young leaves) and six days of submergence (young
542 leaves only), and after 1, 3, and 24 hours of recovery (old and young leaves). RNA was extracted using
543 the Qiagen RNeasy Plant Mini kit, genomic DNA was removed by treating the samples with AMPD1
544 DNase I (Sigma-Aldrich). Libraries were constructed by Macrogen using the TruSeq Stranded mRNA
545 LT Sample Prep Kit (Illumina). Libraries were sequenced on an Illumina NovaSeq6000 platform
546 NovaSeq6000 via paired-end sequencing of 150bp reads. Sequenced libraries were trimmed of adapter
547 sequences using FastQC (Babraham Bioinformatics). Cleaned reads were aligned to the Araport11
548 transcriptome using Kallisto (Bray et al., 2016). Genes were determined as differentially expressed
549 when FDR<0.05 and $|\log_2 FC|>1$, as calculated using R packages EdgeR and limma (Supplemental
550 table 3). Fold changes and p-values for all timepoints were also calculated compared to non-submerged
551 old leaves of Col-0, these were used in Figures S4D and S6A and can be found in Supplemental table
552 4.

553

554 ORE1 binding site density

555 To determine the density of ORE1 binding sites in the promoters of putative target genes, genes were
556 selected from the RNAseq dataset that are induced significantly stronger in Col-0 old leaves than *ore1-*
557 *1* old leaves after 4d of dark submergence. Promoters (1kb upstream and 100bp downstream of the
558 transcriptional start site) of these 287 genes were extracted from the TAIR9 genome sequence using
559 the GenomicRanges R package (Lawrence et al., 2013). These promoters were scanned for the
560 occurrences of the ORE1 motifs $VMGTR_{N5\text{-}6}YACR$ and TDRCGTRHD, allowing one mismatch
561 (Matallana-Ramirez et al., 2013; Olsen et al., 2005). The density of motif centers along the promoter
562 sequences was corrected for the number of scanned promoters and plotted using ggplot2.

563

564 Electrophoretic mobility shift assay

565 EMSAs were performed as previously described by (Wu et al., 2012). ORE1-GST protein was purified
566 as previously described by (Durian et al., 2020). Binding reactions were performed using the Odyssey
567 infrared EMSA kit (LI-COR) following the manufacturer's instructions. DNA-protein complexes were
568 separated in a 6% (w/v) retardation gel (EC6365BOX, Invitrogen). DY682 signal was detected using
569 the Odyssey infrared imaging system from LI-COR.

570 ChIP-qPCR

571 For ChIP, 10-leaf stage Col-0 and *pORE1:ORE1-HA ore1-1* plants were submerged for one day in
572 darkness to induce ORE1-HA protein accumulation. Chromatin was extracted from 1.5g of whole-
573 rosette tissue for each replicate. Protein-DNA complexes were immunoprecipitated using anti-HA
574 antibodies (Miltenyi Biotec) (Kaufmann et al., 2010). After reversion of the cross-linking, DNA was
575 purified with the QIAquick PCR Purification Kit (Qiagen) and was analyzed by qPCR. Enrichment of
576 ORE1 at the target promoters was calculated relative to Col-0, significance was determined by
577 comparing the enrichment at each of the target loci to that of the negative control (AT2G22180).

578 Western blotting

579 Five leaves of the indicated age were pooled together after the indicated treatment and frozen in liquid
580 nitrogen. Protein was extracted using RIPA buffer (Hartman et al., 2019) and quantified using a Pierce
581 BCA kit. 20-50µg of protein was loaded onto a stain-free 4-15% gel (BioRad), the Rubisco large subunit
582 was visualized using stain-free gel imaging. Proteins were transferred from the gel to a 0.2µm PVDF
583 membrane using a Bio-Rad trans-blot system for 7 minutes, efficient transfer was verified by imaging
584 the stain-free blot afterwards. The blot was blocked overnight at 4C in TBS-T + 5% milk. Primary
585 antibody (1:1000, anti-GFP (Roche, #11814460001) or anti-HA-HRP (Thermo Fisher, 26183-HRP))

586 was incubated for 1h @ RT. The blot was washed 4 times 10 minutes with TBS-T. In the case of anti-
587 GFP blots, the membrane was incubated with a secondary antibody (1:2500 rabbit anti-mouse, Cell
588 signaling #7076) for 1h at RT and the membrane was washed 3x with TBS-T and 2x with TBS, 5 minutes
589 each. The membrane was incubated with Femto (Thermo Fisher) and imaged under a ChemiDoc
590 imaging system (BioRad) to visualize HRP activity.

591 To identify phosphorylated proteins, 50µg of protein extract was precipitated by incubating the sample
592 with 4x the volume of the protein sample 100% ice-cold acetone for 1h at -20C. After precipitation the
593 samples were centrifuged for 10 minutes at 13,000g at 4C and the supernatant was removed. The pellet
594 of precipitated proteins was resuspended in 12µl water and 3µl 5x sample loading buffer (250mM Tris
595 (pH 6.8) 25% glycerol, 10% SDS, 0.05% bromophenol blue) containing 5% beta-mercaptoethanol.
596 Samples were boiled for 5 minutes at 95C to denature the proteins and were separated via
597 electrophoresis on a SuperSep Phos-Tag 7.5% gel with 50µmol/l Phos-Tag (198-17981, Fujifilm Wako,
598 Japan). The gel was run at a stable 20mA for 2.5h. After electrophoresis, the gel was washed twice in
599 running buffer containing 10mM EDTA for 10 minutes and once in running buffer without EDTA.
600 Transferring the proteins, blocking the membrane, antibody incubation, and imaging were done
601 identically to non-phostag ORE1-HA Western blots. The large subunit of rubisco was imaged after
602 staining for ORE1-HA using 0.1% (w/v) Ponceau S to verify equal loading.

603 Estradiol treatment

604 Entire *RPS5a::XVE>>ORE1-GFP* plants were sprayed twice daily with 100µM estradiol (from a 20mM
605 estradiol stock in ethanol) in water or a mock solution (0.5% ethanol). Leaves 1, 3, and 7 were harvested
606 after 8 days and snap-frozen in liquid nitrogen.

607 Statistical analysis

608 All statistical tests were done in R version 3.6.1 using the indicated statistical tests, differences were
609 deemed significant at $p<0.05$.

610

611 **Author contributions**

612 Conceptualization: TR, HvV, RS; Investigation: TR, HvV, MS, C-YL, MBD; Data analysis: TR, HvV, MS;
613 Funding acquisition: RS; Methodology: TR, HvV, MS, C-YL; Supervision: SB, RS; Writing – original
614 draft: TR, RS; Writing – review & editing: TR, HvV, SB, RS.

615 **Acknowledgments**

616 We would like to thank Bernhard Würzinger and Markus Teige for their input on PhosTag Western blots
617 and Yorrit van de Kaa for harvesting seeds. This work was financially supported by the Netherlands
618 Organization for Scientific Research grant 016.VIDI.171.006 to TR and RS and grant ALWOP.419 to
619 HvV. SB thanks the Max Planck Institute of Molecular Plant Physiology (MPIMP) and Leiden University
620 for funding.

621 **Data and code availability**

622 RNAseq data has been deposited at the European Nucleotide Archive under accession number
623 PRJEB57289. Transcript abundance in the RNAseq data can also be explored in a Shiny app at
624 https://utrecht-university.shinyapps.io/Rankenberg2022/. All other data and code are available from the
625 lead contact upon request.

626

ReferencesAbbas, M., Berckhan, S., Rooney, D.J., Gibbs, D.J., Vicente Conde, J., Sousa Correia, C., Bassel, G.W., Marín-de la Rosa, N., León, J., Alabadí, D., Blázquez, M.A., and Holdsworth, M.J. (2015). Oxygen Sensing Coordinates Photomorphogenesis to Facilitate Seedling Survival. Current Biology 25: 1483–1488.

Alonso, J.M., Hirayama, T., Roman, G., Nourizadeh, S., and Ecker, J.R. (1999). EIN2, a Bifunctional Transducer of Ethylene and Stress Responses in Arabidopsis. Science 284: 2148–2152.

Alonso, J.M., Stepanova, A.N., Solano, R., Wisman, E., Ferrari, S., Ausubel, F.M., and Ecker, J.R. (2003). Five components of the ethylene-response pathway identified in a screen for weak ethylene-insensitive mutants in Arabidopsis. Proc Natl Acad Sci U S A 100: 2992–2997.

Alpuerto, J.B., Hussain, R.M.F., and Fukao, T. (2016). The key regulator of submergence tolerance, SUB1A, promotes photosynthetic and metabolic recovery from submergence damage in rice leaves. Plant, Cell & Environment 39: 672–684.

Alvarez, J.M., Brooks, M.D., Swift, J., and Coruzzi, G.M. (2021). Time-Based Systems Biology Approaches to Capture and Model Dynamic Gene Regulatory Networks. Annual Review of Plant Biology 72.

Argueso, C.T., Hansen, M., and Kieber, J.J. (2007). Regulation of Ethylene Biosynthesis. J Plant Growth Regul 26: 92–105.

Balazadeh, S., Siddiqui, H., Allu, A.D., Matallana-Ramirez, L.P., Caldana, C., Mehrnia, M., and Mueller-Roeber, B. (2010). A gene regulatory network controlled by the NAC transcription factor ANAC092/AtNAC2/ORE1 during salt-promoted senescence. The Plant Journal 62: 250–264.

Bhaskara, G.B., Wong, M.M., and Verslues, P.E. (2019). The flip side of phospho-signalling: Regulation of protein dephosphorylation and the protein phosphatase 2Cs. Plant, Cell & Environment 42: 2913–2930.

Binder, B.M. (2020). Ethylene signaling in plants. Journal of Biological Chemistry 295: 7710–7725.

Buraschi, F.B., Mollard, F.P.O., Grimoldi, A.A., and Striker, G.G. (2020). Eco-Physiological Traits Related to Recovery from Complete Submergence in the Model Legume Lotus japonicus. Plants 9: 538.

Campbell, M.T., Proctor, C.A., Dou, Y., Schmitz, A.J., Phansak, P., Kruger, G.R., Zhang, C., and Walia, H. (2015). Genetic and Molecular Characterization of Submergence Response Identifies Subtol6 as a Major Submergence Tolerance Locus in Maize. PLOS ONE 10: e0120385.

Cao, X.F., Linstead, P., Berger, F., Kieber, J., and Dolan, L. (1999). Differential ethylene sensitivity of epidermal cells is involved in the establishment of cell pattern in the Arabidopsis root. Physiologia Plantarum 106: 311–317.

Ceusters, J. and Van de Poel, B. (2018). Ethylene exerts species-specific and age-dependent control of photosynthesis. Plant physiology 176: 2601–2612.

Chang, K.N. et al. (2013). Temporal transcriptional response to ethylene gas drives growth hormone cross-regulation in Arabidopsis. eLife 2: e00675.

664 Chao, Q., Rothenberg, M., Solano, R., Roman, G., Terzaghi, W., and Ecker, J.R. (1997). Activation of
665 the Ethylene Gas Response Pathway in Arabidopsis by the Nuclear Protein ETHYLENE-
666 INSENSITIVE3 and Related Proteins. Cell 89: 1133–1144.

667 Chen, L., Dodd, I.C., Davies, W.J., and Wilkinson, S. (2013). Ethylene limits abscisic acid- or soil
668 drying-induced stomatal closure in aged wheat leaves. Plant, Cell and Environment 36:
669 1850–1859.

670 Cheng, S.L.H., Wu, H.-W., Xu, H., Singh, R.M., Yao, T., Jang, I.-C., and Chua, N.-H. (2022). Nutrient
671 status regulates MED19a phase separation for ORESARA1-dependent senescence. New
672 Phytologist.

673 De Rybel, B., van den Berg, W., Lokerse, A., Liao, C.-Y., van Mourik, H., Möller, B., Peris, C.L., and
674 Weijers, D. (2011). A versatile set of ligation-independent cloning vectors for functional
675 studies in plants. Plant Physiology 156: 1292–1299.

676 Doubt, S.L. (1917). The Response of Plants to Illuminating Gas. Botanical Gazette 63: 209–224.

677 Dubois, M., Van den Broeck, L., and Inzé, D. (2018). The Pivotal Role of Ethylene in Plant Growth.
678 Trends in Plant Science 23: 311–323.

679 Durian, G., Sedaghatmehr, M., Matallana-Ramirez, L.P., Schilling, S.M., Schaepe, S., Guerra, T.,
680 Herde, M., Witte, C.-P., Mueller-Roeber, B., Schulze, W.X., Balazadeh, S., and Romeis, T.
681 (2020). Calcium-Dependent Protein Kinase CPK1 Controls Cell Death by In Vivo
682 Phosphorylation of Senescence Master Regulator ORE1. The Plant Cell 32: 1610–1625.

683 Fahlgren, N. et al. (2015). A Versatile Phenotyping System and Analytics Platform Reveals Diverse
684 Temporal Responses to Water Availability in Setaria. Molecular Plant 8: 1520–1535.

685 dela Fuente, R.K. and Leopold, A.C. (1968). Senescence Processes in Leaf Abscission. Plant Physiology
686 43: 1496–1502.

687 Fukao, T. and Bailey-Serres, J. (2008). Submergence tolerance conferred by Sub1A is mediated by
688 SLR1 and SLRL1 restriction of gibberellin responses in rice. Proceedings of the National
689 Academy of Sciences 105: 16814–16819.

690 Fukao, T., Xu, K., Ronald, P.C., and Bailey-Serres, J. (2006). A Variable Cluster of Ethylene Response
691 Factor–Like Genes Regulates Metabolic and Developmental Acclimation Responses to
692 Submergence in Rice. The Plant Cell 18: 2021–2034.

693 Fukao, T., Yeung, E., and Bailey-Serres, J. (2012). The Submergence Tolerance Gene SUB1A Delays
694 Leaf Senescence under Prolonged Darkness through Hormonal Regulation in Rice. Plant
695 Physiology 160: 1795–1807.

696 Gao, Z. et al. (2018). KIRA1 and ORESARA1 terminate flower receptivity by promoting cell death in
697 the stigma of Arabidopsis. Nature Plants 4: 365–375.

698 Garapati, P., Feil, R., Lunn, J.E., Van Dijck, P., Balazadeh, S., and Mueller-Roeber, B. (2015).
699 Transcription Factor Arabidopsis Activating Factor1 Integrates Carbon Starvation Responses
700 with Trehalose Metabolism. Plant Physiology 169: 379–390.

701 Garzón, M., Eifler, K., Faust, A., Scheel, H., Hofmann, K., Koncz, C., Yephremov, A., and Bachmair, A.
702 (2007). PRT6/At5g02310 encodes an Arabidopsis ubiquitin ligase of the N-end rule pathway
703 with arginine specificity and is not the CER3 locus. FEBS Letters 581: 3189–3196.

704 Gibbs, D.J., Lee, S.C., Md Isa, N., Gramuglia, S., Fukao, T., Bassel, G.W., Correia, C.S., Corbineau, F.,
705 Theodoulou, F.L., Bailey-Serres, J., and Holdsworth, M.J. (2011). Homeostatic response to
706 hypoxia is regulated by the N-end rule pathway in plants. Nature 479: 415–418.

707 Graham, L.E., Schippers, J.H.M., Dijkwel, P.P., and Wagstaff, C. (2012). Ethylene and senescence
708 processes. Annual Plant Reviews 44: 305–341.

709 Hartman, S. et al. (2019). Ethylene-mediated nitric oxide depletion pre-adapts plants to hypoxia
710 stress. Nature Communications 10: 4020.

711 Hattori, Y. et al. (2009). The ethylene response factors SNORKEL1 and SNORKEL2 allow rice to adapt
712 to deep water. Nature 460: 1026–1030.

713 Havé, M., Marmagne, A., Chardon, F., and Masclaux-Daubresse, C. (2017). Nitrogen remobilization
714 during leaf senescence: lessons from Arabidopsis to crops. Journal of Experimental Botany
715 68: 2513–2529.

716 He, X.-J., Mu, R.-L., Cao, W.-H., Zhang, Z.-G., Zhang, J.-S., and Chen, S.-Y. (2005). AtNAC2, a
717 transcription factor downstream of ethylene and auxin signaling pathways, is involved in salt
718 stress response and lateral root development. Plant J 44: 903–916.

719 Jing, H.-C., Schippers, J.H.M., Hille, J., and Dijkwel, P.P. (2005). Ethylene-induced leaf senescence
720 depends on age-related changes and OLD genes in Arabidopsis. Journal of Experimental
721 Botany 56: 2915–2923.

722 Kaufmann, K., Muiño, J.M., Østerås, M., Farinelli, L., Krajewski, P., and Angenent, G.C. (2010).
723 Chromatin immunoprecipitation (ChIP) of plant transcription factors followed by sequencing
724 (ChIP-SEQ) or hybridization to whole genome arrays (ChIP-CHIP). Nature Protocols 5: 457–
725 472.

726 Kim, C., Kim, S.J., Jeong, J., Park, E., Oh, E., Park, Y.-I., Lim, P.O., and Choi, G. (2020). High Ambient
727 Temperature Accelerates Leaf Senescence via PHYTOCHROME-INTERACTING FACTOR 4 and
728 5 in Arabidopsis. Molecules and Cells 43: 645–661.

729 Kim, G.-D., Cho, Y.-H., and Yoo, S.-D. (2017). Regulatory Functions of Cellular Energy Sensor SNF1-
730 Related Kinase1 for Leaf Senescence Delay through ETHYLENE- INSENSITIVE3 Repression.
731 Scientific Reports 7: 3193.

732 Kim, H.J., Park, J.H., Kim, J., Kim, J.J., Hong, S., Kim, J., and Nam, H.G. (2018). Time-evolving genetic
733 networks reveal a NAC troika that negatively regulates leaf senescence in *Arabidopsis*.
734 Proceedings of the National Academy of Sciences 115: 4930–4939.

735 Kim, J.H., Woo, H.R., Kim, J., Lim, P.O., Lee, I.C., Choi, S.H., and Nam, H.G. (2009). Trifurcate feed-
736 forward regulation of age-dependent cell death involving *miR164* in *Arabidopsis*. Science
737 323: 1053–1057.

738 Krishnan, P., Ravi, I., and Rama Krishnayya, G. (1999). Leaf Senescence in Submerged Rice Plants.
739 Experimental Agriculture 35: 345–355.

740 Kuroha, T. et al. (2018). Ethylene-gibberellin signaling underlies adaptation of rice to periodic
741 flooding. Science 361: 181–186.

742 Lawrence, M., Huber, W., Pagès, H., Aboyoun, P., Carlson, M., Gentleman, R., Morgan, M.T., and
743 Carey, V.J. (2013). Software for Computing and Annotating Genomic Ranges. PLOS
744 Computational Biology 9: e1003118.

745 Li, Z., Peng, J., Wen, X., and Guo, H. (2013). *ETHYLENE-INSENSITIVE3* is a senescence-associated gene
746 that accelerates age-dependent leaf senescence by directly repressing *miR164* transcription
747 in *Arabidopsis*. Plant Cell 25: 3311–3328.

748 Lin, C.-C. et al. (2019). Regulatory cascade involving transcriptional and N-end rule pathways in rice
749 under submergence. Proceedings of the National Academy of Sciences 116: 3300–3309.

750 Liu, Z. et al. (2022). Ethylene augments root hypoxia tolerance via growth cessation and reactive
751 oxygen species amelioration. Plant Physiology 190: 1365–1383.

752 Logemann, E., Birkenbihl, R.P., Ülker, B., and Somssich, I.E. (2006). An improved method for
753 preparing Agrobacterium cells that simplifies the Arabidopsis transformation protocol. Plant
754 Methods 2: 16.

755 Masson, N., Keeley, T.P., Giuntoli, B., White, M.D., Puerta, M.L., Perata, P., Hopkinson, R.J.,
756 Flashman, E., Licausi, F., and Ratcliffe, P.J. (2019). Conserved N-terminal cysteine
757 dioxygenases transduce responses to hypoxia in animals and plants. Science 365: 65–69.

758 Matallana-Ramirez, L.P., Rauf, M., Farage-Barhom, S., Dortay, H., Xue, G.-P., Dröge-Laser, W., Lers,
759 A., Balazadeh, S., and Mueller-Roeber, B. (2013). NAC transcription factor ORE1 and
760 senescence-induced BIFUNCTIONAL NUCLEASE1 (BFN1) constitute a regulatory cascade in
761 Arabidopsis. Molecular Plant 6: 1438–1452.

762 Métraux, J.-P. and Kende, H. (1983). The Role of Ethylene in the Growth Response of Submerged
763 Deep Water Rice. Plant Physiology 72: 441–446.

764 Mustroph, A., Zanetti, M.E., Jang, C.J., Holtan, H.E., Repetti, P.P., Galbraith, D.W., Girke, T., and
765 Bailey-Serres, J. (2009). Profiling translatomes of discrete cell populations resolves altered
766 cellular priorities during hypoxia in Arabidopsis. Proceedings of the National Academy of
767 Sciences 106: 18843–18848.

768 Nagahage, I.S.P., Sakamoto, S., Nagano, M., Ishikawa, T., Kawai-Yamada, M., Mitsuda, N., and
769 Yamaguchi, M. (2018). An NAC domain transcription factor ATAF2 acts as transcriptional
770 activator or repressor dependent on promoter context. Plant Biotechnology 35: 285–289.

771 Olsen, A.N., Ernst, H.A., Leggio, L.L., and Skriver, K. (2005). DNA-binding specificity and molecular
772 functions of NAC transcription factors. Plant Science 169: 785–797.

773 Park, B.S., Yao, T., Seo, J.S., Wong, E.C.C., Mitsuda, N., Huang, C.-H., and Chua, N.-H. (2018).
774 Arabidopsis NITROGEN LIMITATION ADAPTATION regulates ORE1 homeostasis during
775 senescence induced by nitrogen deficiency. Nature Plants 4: 898–903.

776 Park, S.-H., Jeong, J.S., Seo, J.S., Park, B.S., and Chua, N.-H. (2019). Arabidopsis ubiquitin-specific
777 proteases UBP12 and UBP13 shape ORE1 levels during leaf senescence induced by nitrogen
778 deficiency. New Phytologist 223: 1447–1460.

779 Peng, H.-P., Chan, C.-S., Shih, M.-C., and Yang, S.F. (2001). Signaling Events in the Hypoxic Induction
780 of Alcohol Dehydrogenase Gene in Arabidopsis. Plant Physiology 126: 742–749.

781 Podzimska-Sroka, D., O'Shea, C., Gregersen, P.L., and Skriver, K. (2015). NAC Transcription Factors in
782 Senescence: From Molecular Structure to Function in Crops. Plants 4: 412–448.

783 Polko, J.K., Voesenek, L.A.C.J., Peeters, A.J.M., and Pierik, R. (2011). Petiole hyponasty: an ethylene-
784 driven, adaptive response to changes in the environment. AoB PLANTS 2011: plr031.

785 Qiu, K., Li, Z., Yang, Z., Chen, J., Wu, S., Zhu, X., Gao, S., Gao, J., Ren, G., Kuai, B., and Zhou, X. (2015).
786 EIN3 and ORE1 Accelerate Degreening during Ethylene-Mediated Leaf Senescence by
787 Directly Activating Chlorophyll Catabolic Genes in Arabidopsis. PLOS Genetics 11: e1005399.

788 Rajhi, I., Yamauchi, T., Takahashi, H., Nishiuchi, S., Shiono, K., Watanabe, R., Mliki, A., Nagamura, Y.,
789 Tsutsumi, N., Nishizawa, N.K., and Nakazono, M. (2011). Identification of genes expressed in
790 maize root cortical cells during lysigenous aerenchyma formation using laser microdissection
791 and microarray analyses. New Phytologist 190: 351–368.

792 Rankenberg, T., Geldhof, B., van Veen, H., Holsteens, K., Van de Poel, B., and Sasidharan, R. (2021).
793 Age-Dependent Abiotic Stress Resilience in Plants. Trends in Plant Science 26: 692–705.

794 Rauf, M., Arif, M., Fisahn, J., Xue, G.-P., Balazadeh, S., and Mueller-Roeber, B. (2013). NAC
795 Transcription Factor SPEEDY HYPONASTIC GROWTH Regulates Flooding-Induced Leaf
796 Movement in Arabidopsis. The Plant Cell 25: 4941–4955.

797 Sakuraba, Y., Jeong, J., Kang, M.Y., Kim, J., Paek, N.C., and Choi, G. (2014). Phytochrome-interacting
798 transcription factors PIF4 and PIF5 induce leaf senescence in Arabidopsis. Nature
799 Communications 5: 4636.

800 Sasidharan, R., Hartman, S., Liu, Z., Martopawiro, S., Sajeev, N., van Veen, H., Yeung, E., and
801 Voesenek, L.A. (2018). Signal dynamics and interactions during flooding stress. Plant
802 physiology 176: 1106–1117.

803 Sasidharan, R. and Voesenek, L.A.C.J. (2015). Ethylene-Mediated Acclimations to Flooding Stress.
804 Plant Physiology 169: 3–12.

805 Shi, H., Shen, X., Liu, R., Xue, C., Wei, N., Deng, X.W., and Zhong, S. (2016). The Red Light Receptor
806 Phytochrome B Directly Enhances Substrate-E3 Ligase Interactions to Attenuate Ethylene
807 Responses. Developmental Cell 39: 597–610.

808 Simeunovic, A., Mair, A., Wurzinger, B., and Teige, M. (2016). Know where your clients are:
809 subcellular localization and targets of calcium-dependent protein kinases. Journal of
810 Experimental Botany 67: 3855–3872.

811 Stepanova, A.N. and Alonso, J.M. (2009). Ethylene signaling and response: where different
812 regulatory modules meet. Current Opinion in Plant Biology 12: 548–555.

813 Tsai, K.-J., Chou, S.-J., and Shih, M.-C. (2014). Ethylene plays an essential role in the recovery of
814 Arabidopsis during post-anaerobiosis reoxygenation. Plant, Cell & Environment 37: 2391–
815 2405.

816 Vandenbussche, F., Vaseva, I., Vissenberg, K., and Van Der Straeten, D. (2012). Ethylene in vegetative
817 development: a tale with a riddle. 194: 895–909.

818 Vaseva, I.I., Qudeimat, E., Potuschak, T., Du, Y., Genschik, P., Vandenbussche, F., and Van Der
819 Straeten, D. (2018). The plant hormone ethylene restricts Arabidopsis growth via the
820 epidermis. Proceedings of the National Academy of Sciences 115: E4130–E4139.

821 Vashisht, D., Hesselink, A., Pierik, R., Ammerlaan, J.M.H., Bailey-Serres, J., Visser, E.J.W., Pedersen,
822 O., van Zanten, M., Vreugdenhil, D., Jamar, D.C.L., Voesenek, L. a. C.J., and Sasidharan, R.
823 (2011). Natural variation of submergence tolerance among Arabidopsis thaliana accessions.
824 New Phytologist 190: 299–310.

825 Voesenek, L.A.C.J. and Sasidharan, R. (2013). Ethylene – and oxygen signalling – drive plant survival
826 during flooding. Plant Biology 15: 426–435.

827 Weits, D.A., Kunkowska, A.B., Kamps, N.C.W., Portz, K.M.S., Packbier, N.K., Nemec Venza, Z.,
828 Gaillochet, C., Lohmann, J.U., Pedersen, O., Dongen, J.T., and Licausi, F. (2019). An apical
829 hypoxic niche sets the pace of shoot meristem activity. Nature 569: 714–717.

830 Woo, H.R., Kim, H.J., Lim, P.O., and Nam, H.G. (2019). Leaf senescence: Systems and dynamics
831 aspects. Annual review of plant biology 70: 347–376.

832 Wu, A., Allu, A.D., Garapati, P., Siddiqui, H., Dortay, H., Zanor, M.I., and Fernie, A.R. (2012).
833 *JUNGBRUNNEN1*, a reactive oxygen species–responsive NAC transcription factor, regulates
834 longevity in *Arabidopsis*. The Plant Cell 24: 482–506.

835 Xie, L.-J. et al. (2015). Unsaturation of Very-Long-Chain Ceramides Protects Plant from Hypoxia-
836 Induced Damages by Modulating Ethylene Signaling in Arabidopsis. PLOS Genetics 11:
837 e1005143.

838 Xu, K., Xu, X., Fukao, T., Canlas, P., Maghirang-Rodriguez, R., Heuer, S., Ismail, A.M., Bailey-Serres, J.,
839 Ronald, P.C., and Mackill, D.J. (2006). Sub1A is an ethylene-response-factor-like gene that
840 confers submergence tolerance to rice. Nature 442: 705–708.

841 Xue, H., Jingjing, M., Pei, L., Cao, Y., An, X., Jia, M., Li, Y., Liu, H., Sheen, J., Liu, X., and Yu, F. (2022).
842 ARF2-PIF5 interaction controls transcriptional reprogramming in the ABS3-mediated plant
843 senescence pathway. The EMBO Journal: e110988.

844 Yanagisawa, S., Yoo, S.-D., and Sheen, J. (2003). Differential regulation of EIN3 stability by glucose
845 and ethylene signalling in plants. Nature 425: 521–525.

846 Yeung, E. et al. (2018). A stress recovery signaling network for enhanced flooding tolerance in
847 Arabidopsis thaliana. Proceedings of the National Academy of Sciences 115: E6085–E6094.

848 Yu, Y., Qi, Y., Xu, J., Dai, X., Chen, J., Dong, C.-H., and Xiang, F. (2021). Arabidopsis WRKY71 regulates
849 ethylene-mediated leaf senescence by directly activating EIN2, ORE1 and ACS2 genes. The
850 Plant Journal 107: 1819–1836.

851 Zhang, J., Toai, T.V., Huynh, L., and Preiszner, J. Development of flooding-tolerant Arabidopsis
852 thaliana by autoregulated cytokinin production.: 10.

853 Zhang, Y., Gao, Y., Wang, H.-L., Kan, C., Li, Z., Yang, X., Yin, W., Xia, X., Nam, H.G., Li, Z., and Guo, H.
854 (2021). Verticillium dahliae secretory effector PevD1 induces leaf senescence by promoting
855 ORE1-mediated ethylene biosynthesis. Molecular Plant: S1674-2052(21)00280-X.

856 Zhong, S., Shi, H., Xue, C., Wang, L., Xi, Y., Li, J., Quail, P.H., Deng, X.W., and Guo, H. (2012). A
857 Molecular Framework of Light-Controlled Phytohormone Action in Arabidopsis. Current
858 Biology 22: 1530–1535.

859